

Graph Cuts-Based Registration Revisited: A Novel Approach for Lung Image Registration Using Supervoxels and Image-Guided Filtering

Adam Szmul¹, Bartłomiej W. Papież¹, Russell Bates¹, Andre Hallack¹,
Julia A. Schnabel^{1,2}, Vicente Grau¹

¹Institute of Biomedical Engineering, Department of Engineering Science,
University of Oxford, UK

²Department of Biomedical Engineering, Division of Imaging Sciences and Biomedical Engineering,
King's College London, UK

adam.szmul@eng.ox.ac.uk

Abstract

This work revisits the concept of graph cuts as an efficient optimization technique in image registration. Previously, due to the computational burden involved, the use of graph cuts in this context has been mainly limited to 2D applications. Here we show how combining graph cuts with supervoxels, resulting in a sparse, yet meaningful graph-based image representation, can overcome previous limitations. Additionally, we show that a relaxed graph representation of the image allows for ‘sliding’ motion modeling and provides anatomically plausible estimation of the deformations. This is achieved by using image-guided filtering of the estimated sparse deformation field. We evaluate our method on a publicly available CT lung data set and show that our new approach compares very favourably with state-of-the-art in continuous and discrete image registration.

Keywords: *graph cuts, discrete optimization, image registration, supervoxels, image-guided filtering*

1. Introduction

Image registration, especially for medical applications, remains an active and challenging field of research. One of the most demanding applications of image registration is lung registration, particularly because of the ‘sliding’ motion between the lungs and surrounding tissues that makes conventional regularisers unsuited to the task. Lung registration is important for radiotherapy planning [19], treatment monitoring [36] and ventilation quantification [9]. This paper addresses single-modality intra-patient lung Computed Tomography (CT) registration, which is especially important in radiotherapy planning.

Several methods have been proposed and evaluated in [22]. In general they can be divided into two groups, with respect to the optimization method: continuous [21] and discrete [13].

In this paper, we focus on the latter type of optimization, which is becoming increasingly popular in medical image analysis, and present a novel medical image registration approach that successfully combines graph cuts-based optimization with supervoxel image representation and image-guided filtering. Additionally, we propose to apply the graph cuts method on a relaxed graph formulation, which helps to preserve lung ‘sliding’ motion at lung borders, while at the same time ensuring sufficient regularization inside and outside of the lungs.

This paper is structured as follows. In the following Section 2 we introduce discrete optimization as a platform for image registration, before presenting the supervoxel image clustering method. In Section 3 the proposed framework is discussed in detail, while in Section 4, we show the experimental set-up and results obtained for the proposed framework applied to lung CT image volumes. The results are discussed in Section 5, where we compare them against results achieved by the most closely related methods in the field: bilateral filtering Demons-based [24], dense displacement sampling method [17] and supervoxel-belief propagation [18]. The paper is summarized in Section 6 and provides an overview on our future work plans.

2. Background

2.1. Lung image registration

There are a number of remaining challenges in lung registration which make this an active field of research. One of them is dealing with ‘sliding’ motion between organs, in particular on the surface of the lung pleura. In order to ad-

dress this issue, the deformation field should, in general, be smooth but local discontinuities should be allowed. Conventional registration methods, providing a smooth deformation field across the whole image, do not model well this complex issue.

The particular problem has been a topic of interest for a number of studies. In [28], the authors proposed to decouple diffusion regularization into normal and tangential directions around the lung boundaries using automatically detected masks. A similar approach was used in [3] for Positron Emission Tomography (PET) to CT image registration. A piecewise diffeomorphism, as an extension to Large Deformation Diffeomorphic Metric Mapping (LDDMM), was proposed in [25]. Bilateral filtering as regularization of the deformation field, preserving ‘sliding’ motion, was proposed in [24]. In [17], Heinrich *et al.* proposed a Markov Random Field (MRF) based approach, where, apart from accurate lung registration, ventilation maps can be estimated. Recently, a symmetric regularized correspondence fields method was introduced in [15] for images from patients with Chronic Obstructive Pulmonary Disease (COPD) and supervoxel-based belief propagation algorithm in [18].

2.2. MRFs and graph cuts for image registration

Image registration is the process of finding an optimal transformation between two images. The problem can be stated as an MRF-based optimization task, where, in contrast to continuous optimization methods, only predefined discrete displacements are allowed. Then the optimization can be formulated on an undirected graph with a set of nodes, P , and used to solve a labelling problem, where every node $p \in P$ must be assigned a label f_p from a finite label set \mathcal{L} . Here the labels represent a displacement vector, which allows the use of MRFs in image registration algorithms. The MRF labelling problem can be formulated as an optimization process, consisting of data and piecewise smoothness terms:

$$E(f) = E_{data}(f) + \kappa E_{smooth}(f) \quad (1)$$

where $E_{data}(f)$ represents the disagreement between labelling f and the observed data, $E_{smooth}(f)$ is a piecewise smoothness term and κ is a weighting factor determining the influence of the smoothness term. In most applications it is expected that the labels representing displacement vectors change smoothly across the image. However, in some regions, dramatic changes in the labelling should be allowed. In the case of lung registration, for example, these changes are located at the surface of the lungs and rib cage, where ‘sliding’ motion of the lungs occur. Thus, Eq. 1 can be formulated as:

$$E(f) = \sum_{p \in P} (D_p(f_p)) + \kappa \sum_{p, q \in N} (V_{p, q}(f_p, f_q)) \quad (2)$$

where $D_p(f_p)$ describes N is a subset of P and represents a direct neighbourhood of the current node, p and $V_{p, q}(f_p, f_q)$ is a potential between each pair of neighbouring nodes, p and q , penalizing differences between their respective labels, f_p and f_q , which has the effect of regularizing the transformation. Such a formulation of an energy function to be optimized was presented in [12], where the authors proposed to use linear programming as a solver in image registration. Belief propagation, with its tree-based simplified version [11], has been successfully applied to medical image registration in [17]. The method of graph cuts is another very popular approach to solve a range of optimization problems in computer vision. Since its introduction in [7], the method has been successfully applied to image segmentation [4], stereo matching [5], image restoration and object classification [6]. As we are estimating the displacement field, the problem can be considered as a segmentation and solved in efficient way using this method. Graph cuts were originally proposed as a method to solve a binary labelling problem. They were further generalised as a method applicable to multi-label problems by α -expansion and $\alpha - \beta$ -swap variants. However, α -expansion can only be applied when the piecewise smoothness term is a metric. $\alpha - \beta$ -swap is an iterative optimization method, where for a randomly chosen pair of labels α and β from \mathcal{L} , the global energy in Eq. 2 is minimized by changing the label assignment to a node from α to β and vice versa. Such an operation is called a swap move and solves a binary problem for every pair of labels.

The method of graph cuts has been proposed as a framework for non-linear medical image registration in [32] and enhanced by using a landmark-based approach [20], mutual information as a similarity measure [29] or using a prior joint intensity distribution [30]. In these applications the piecewise smoothness term was calculated as a difference between first-order derivatives of the deformation field. However, the experiments were limited only to 2D brain and coronary angiogram images, except in [32], where the method was applied to 3D brain volumes. Furthermore, the method of graph cuts was applied to 3D medical image registration in [31] (with the sum of absolute differences (SAD) as a similarity measure). However, reported long computation time (up to 25 hours, depending on number of labels used) has, to-date, limited its wider usage in medical imaging. This is due to the high complexity of the problem, which is proportional to the number of voxels and the number of labels in \mathcal{L} . In this work we overcome these computational limitations by using a sparse image representation based on the concept of supervoxels.

2.3. Supervoxel image representation

To reduce the dimensionality of the discrete registration problem, where a displacement vector is calculated for each

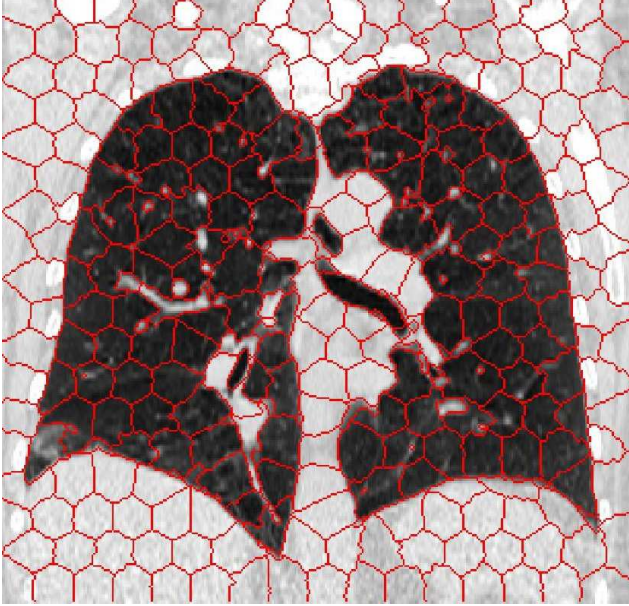


Figure 1. An example of superpixel image representation on a lung coronal slice from Dir-Lab case 8. The superpixels correspond well with lung boundaries and airways inside lungs. For illustrative purposes, we use 2D superpixels and present them on a 2D slice. However, in the framework we extract supervoxels from 3D volumes.

individual voxel, the parameterization of an image on a regular grid is a common solution. However, when a regular grid is applied, it usually does not correspond well with underlying anatomical structures, and regularization across their borders could occur. To overcome this limitation, we follow an approach of supervoxel image clustering, where an image is over-segmented into smaller regions, based on spatial and intensity distance. Recently, an image registration approach with multiple layers of supervoxels with minimum spanning tree (MST) message passing algorithm [18] and adaptive over-segmentation method [23] using supervoxels in regularization step were proposed. The following section presents in detail the proposed framework for lung image registration.

3. Methods

In this section, we present our new framework for lung registration. We start by introducing the chosen supervoxel image representation method in Section 3.1, explain graph cuts as a method for solving MRFs in Section 3.2, provide details about the used similarity measure in Section 3.3 and present the image-guided filtering method in Section 3.4. We finalise by explaining the symmetric formulation of the framework in Section 3.5.

3.1. SLIC clustering

The proposed framework applies Simple Linear Iterative Clustering (SLIC) [1] as a clustering method, due to its speed of performance, direct control over the number of extracted supervoxels and supervoxel compactness. The SLIC method is designed to extract k approximately equally-sized supervoxels, where k is the desired number of supervoxels. It starts by distributing seeds for each of the supervoxels, initially placed at intervals $S = \sqrt[3]{M/k}$ voxels apart, with M being the total number of voxels in the image. The positions of the centers are then corrected based on the gradients of the image to avoid locating them on image edges or at a noisy voxel before each voxel is assigned to the nearest cluster. In an iterative procedure, the distance between each voxel \mathbf{x} and the closest cluster center \mathbf{c} is calculated based on the Euclidean distance $d_e = \|\mathbf{x} - \mathbf{c}\|$ and the intensity-based similarity is $d_I = \sqrt{(I(\mathbf{x}) - I(\mathbf{c}))^2}$. The distance \mathcal{I} is defined as follows:

$$\mathcal{I} = \sqrt{(d_e)^2 + \left(\frac{d_I}{S}\right)^2 m^2}, \quad (3)$$

where m is a parameter corresponding to compactness of supervoxels.

Using such a formulation, we can extract supervoxels from the images. An example of such an over-segmentation on one of the lung images is illustrated in Figure 1.

3.2. Graph cuts

Our optimization problem is posed on an undirected graph, defined by the adjacency of previously extracted supervoxels. Every pair of directly neighbouring supervoxels is connected by an edge. Values of the edges are calculated based on the absolute difference between mean intensities of the supervoxels. In our approach we propose to use a relaxed form of the graph, assuming that in the previously formulated graph, the edges with high value connect inhomogeneous structures and can thus be removed, based on a relaxation threshold parameter v . Such a formulation additionally encourages discontinuities to appear at the lung boundaries, while at the same time preserving the continuous deformation field inside them.

Our formulation builds on graph-based regularization [23] and shares some aspects of the minimum spanning tree (MST)-based belief propagation proposed in [17]. This approach has the advantage of eliminating only edges that connect supervoxels from inconsistent regions, while preserving all connections inside homogeneous structures. The proposed formulation should result in more physically plausible regularization inside the lungs and, in turn, a more realistic deformation field. The introduced relaxation of the graph can be considered as a form of pre-segmentation of the image, akin to lung masking, which is common practice [25, 27, 34].

The data cost term is formulated as a mean error calculated for all voxels \mathbf{x} in the fixed I_{fix} and moving I_{mov} images clustered in a certain supervoxel represented by a node p , for the applied displacement f_p :

$$E_{data}(f) = \Sigma_p (|I_{fix}(\mathbf{x}_p) - I_{mov}(\mathbf{x}_p + f_p)|), \quad (4)$$

The piecewise smoothness term can take one of a number of forms. In the simplest Potts model, the term takes the value 1 when labels are equal and 0 otherwise. In a linear model, the smoothness term value changes linearly according to the distance between labels. The most common way of formulating regularization in image registration is by a quadratic model, which depends on the squared difference between label distances. The first two formulations of the piecewise smoothness term satisfy all metric requirements, including the triangle inequality. In our formulation, we propose to use the following piecewise smoothness term:

$$E_{smooth}(f) = \Sigma_{p,q \in N} \frac{\|f_p - f_q\|^2}{\|I_{mov}(\mathbf{x}_p) - I_{mov}(\mathbf{x}_q)\|}, \quad (5)$$

where the denominator represents the edge values of the graph.

On such formulated problem we apply the graph cuts method [7]. Due to the fact that we are using a quadratic regularization term, which does not satisfy a metric condition about the triangle inequality, we use $\alpha - \beta$ -swap variant of the graph cuts method, which has relaxed requirements about piecewise smoothness term properties and can be used with a semi-metric piecewise smoothness term.

3.3. Similarity measure

The most commonly used similarity measures, based purely on differences between intensities of corresponding voxels, such as sum of absolute differences (SAD) or sum of squared differences (SSD), have their well-known limitations when applied to lung registration. Due to changes in lung tissue density during breathing, the corresponding regions of the lungs at different breathing phases can vary in intensity. To address this issue, we use the modality independent descriptor (MIND) [16] as a similarity measure, which has been originally developed for lung registration. This descriptor calculates for every voxel a vector describing how similar that voxel is to its neighbours. The main advantage of MIND is that it provides a descriptor which is sensitive to similarities in gradients and texture, and much less susceptible to differences in intensities. Thus, the data term from Eq. 4 calculates the mean absolute difference between descriptors and takes the form:

$$E_{data}(f) = \Sigma_p (|\text{MIND}(I_{fix}) - \text{MIND}(I_{mov}(f_p))|), \quad (6)$$

where $\text{MIND}(I_{fix})$ and $\text{MIND}(I_{fix}(f_p))$ are respectively the descriptors calculated for the fixed image and the moving image after applying the displacements represented by labelling f .

3.4. Image-guided filtering

A direct application of the estimated sparse displacement field on a parameterized image would result in discontinuous and physiologically implausible deformations. To overcome this limitation, in [18] the authors proposed using multiple layers of supervoxels while in [12, 17] free-form deformation (FFD) with B-splines [26] is used as an interpolation method. However, the properties of B-splines do not allow us to model discontinuities of the deformation field, which occur between the lungs, rib cage and diaphragm.

We apply an alternative solution: image-guided filtering [14], where an output image I_{out} is a linear combination of an input image I_{in} and an image used as a guide, I_g :

$$I_{out}(\mathbf{x}) = \Sigma_{\mathbf{y} \in \mathcal{N}(\mathbf{x})} \mathbf{W}_{\mathbf{y}}(I_g) I_{in}(\mathbf{y}), \quad (7)$$

where $\mathbf{W}_{\mathbf{y}}$ is a filter kernel calculated for the guide image I_g in a neighbourhood $\mathcal{N}(\mathbf{x})$ of a voxel \mathbf{x} . The kernel $\mathbf{W}_{\mathbf{y}}$ is defined as:

$$\mathbf{W}_{\mathbf{y}}(I_g) = 1 + (I_g - \mu_{I_g})^T (I_g - \mu_{I_g}) (cov_{I_g} + \sigma \mathbf{I})^{-1}, \quad (8)$$

where μ_{I_g} , cov_{I_g} are the mean and covariance of the guidance image I_g calculated in a neighbourhood $\mathcal{N}(\mathbf{x})$, \mathbf{I} is the identity matrix and σ is the smoothness parameter. In our method, this filter is applied over the sparse displacement field T using the moving image I_{mov} as a guide. This yields smooth deformations across anatomically consistent regions in the moving image, while at the same time preserves discontinuities in the deformation field at the region boundaries. The idea of image-guided filtering is based on the edge-preserving approach, similar to bilateral filtering [33], which discourages smoothing across boundaries. Both methods, bilateral filtering and image-guided filtering have good edge-preserving smoothing properties. The main benefit of image-guided filtering is that it is several times faster than bilateral filtering. Related approaches that were previously proposed include continuous optimization-based registration in the lungs [24], where bilateral filtering was applied, and liver motion compensation [23] with image-guided filtering.

3.5. Symmetric formulation

A symmetric formulation of image registration [2] is applied to include more information about the complex nature of the lungs during breathing. At each resolution level, two deformation fields are calculated: from the moving image to the target and vice versa. This is advantageous as the choice of the target and source image does not bias the results of the registration. Additionally, the symmetric formulation partly compensates for discontinuities in the estimated deformation field originating from the relaxed graph formulation. After performing an optimization at each resolution

Error in [mm] and standard deviation					
Case	Initial	Proposed	BLF [24]	deeds [17]	SBP [18]
c1	3.89 ± 2.8	1.00±0.5	1.05 ± 0.5	0.97 ± 0.5	1.19 ± 0.6
c2	4.34 ± 3.9	0.96±0.5	1.08 ± 0.6	0.96 ± 0.5	1.01 ± 0.6
c3	6.94 ± 4.0	1.13±0.6	1.49 ± 0.9	1.21 ± 0.7	1.20 ± 0.6
c4	9.83 ± 4.8	1.39±0.9	1.90 ± 1.3	1.39 ± 1.0	1.36 ± 0.9
c5	7.48 ± 5.5	1.36±1.3	1.99 ± 1.7	1.72 ± 1.6	1.42 ± 1.3
c6	10.9 ± 6.9	1.16±0.6	2.36 ± 1.9	1.49 ± 1.0	1.22 ± 0.7
c7	11.0 ± 7.4	1.17±0.7	2.32 ± 1.9	1.58 ± 1.2	1.27 ± 0.7
c8	15.0 ± 9.0	1.29±1.2	3.58 ± 3.4	2.11 ± 2.4	1.26 ± 0.9
c9	7.92 ± 3.9	1.20±0.6	1.74 ± 1.0	1.36 ± 0.7	1.20 ± 0.7
c10	7.3 ± 6.3	1.19±0.8	2.02 ± 2.1	1.55 ± 1.6	1.23 ± 0.8
Mean	8.46 ± 5.4	1.18±0.8	1.95 ± 0.7	1.43 ± 1.3	1.23 ± 0.8

Table 1. Comparison of the proposed method with the closest implementations based on mean TRE and standard deviations for Dir-Lab data set. For each case, the TRE (stdev) before registration (Initial) and after registration are shown: our proposed method, after bilateral-filtering combined with Demons (BLF [24]), after the dense displacement sampling method based on belief propagation on a minimum spanning tree (deeds [17]), and after supervoxel-based belief propagation (SBP [18]). Best results are shown in bold. Mean results show that our proposed method outperforms all of the compared methods in average.

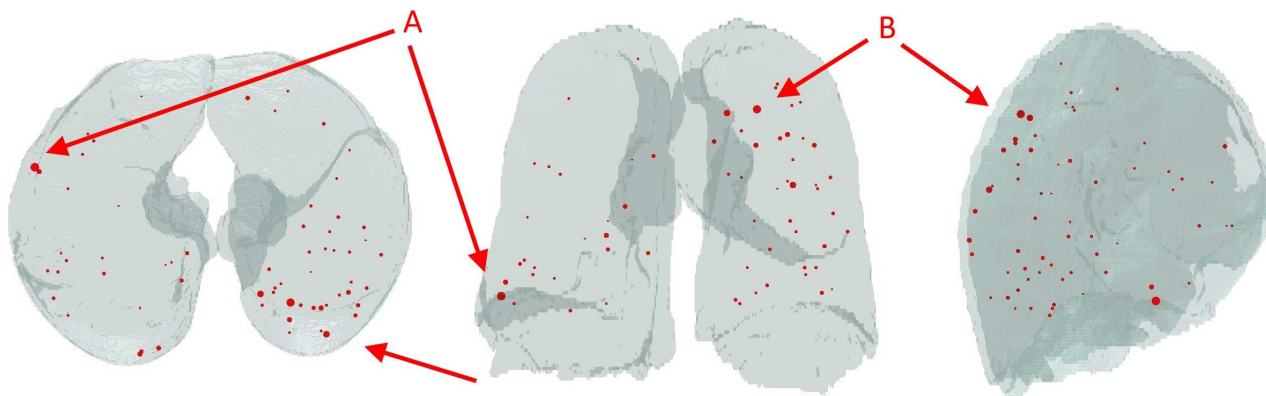


Figure 2. Distribution of the landmark error for the most challenging case 8 after registration in all three views with the lung mask in the background. Only landmarks with error higher than 1.2mm are displayed. The size of the points corresponds with the landmark error. It can be noticed that the biggest errors (pointed by arrows in red) occur in the bottom corner of the lungs - A (16.3mm), which correspond to an artefact shown in Figure 3, and close to the lung borders - B (10.7mm), which imply that ‘sliding’ motion in this region is not sufficient.

level, inverse transformations of both previously calculated transformations are approximated based on a simple fixed-point approach originally proposed in [10] and combined with the corresponding forward transformations.

$$T_{f \rightarrow m}^{new} = (T_{f \rightarrow m} + T_{m \rightarrow f}^{-1}) \cdot (0.5), \quad (9)$$

$$T_{m \rightarrow f}^{new} = (T_{m \rightarrow f} + T_{f \rightarrow m}^{-1}) \cdot (0.5), \quad (10)$$

where $T_{m \rightarrow f}$ and $T_{f \rightarrow m}$ stand for transformations from I_{mov} to I_{fix} and from I_{fix} to I_{mov} respectively.

4. Experiments and Results

The proposed framework was evaluated on the publicly available Dir-Lab dataset [8], which consists of 10 cases of

4D CT lung data with spatial resolution varying between $0.97 \times 0.97 \times 2.5$ and $1.16 \times 1.16 \times 2.5 \text{ mm}^3$. For each individual case, 300 manually placed landmarks in full inhale and full exhale images were provided.

In the conducted experiments we used 5 resolution levels with different numbers of voxels assigned to each supervoxel: 100, 150, 400, 700, 400. The maximum allowed displacement was $\mathcal{M} = \{3, 3.5, 3.75, 4, 2\}$ voxels and displacements were discretized at intervals of size $d = \{0.5, 0.5, 0.75, 1, 0.5\}$ voxels respectively. The image-guided filter window was defined as $w = [5 \ 5 \ 5]$ and the smoothness parameter σ was set to 0.001. The graph relaxation threshold parameter v was empirically chosen as

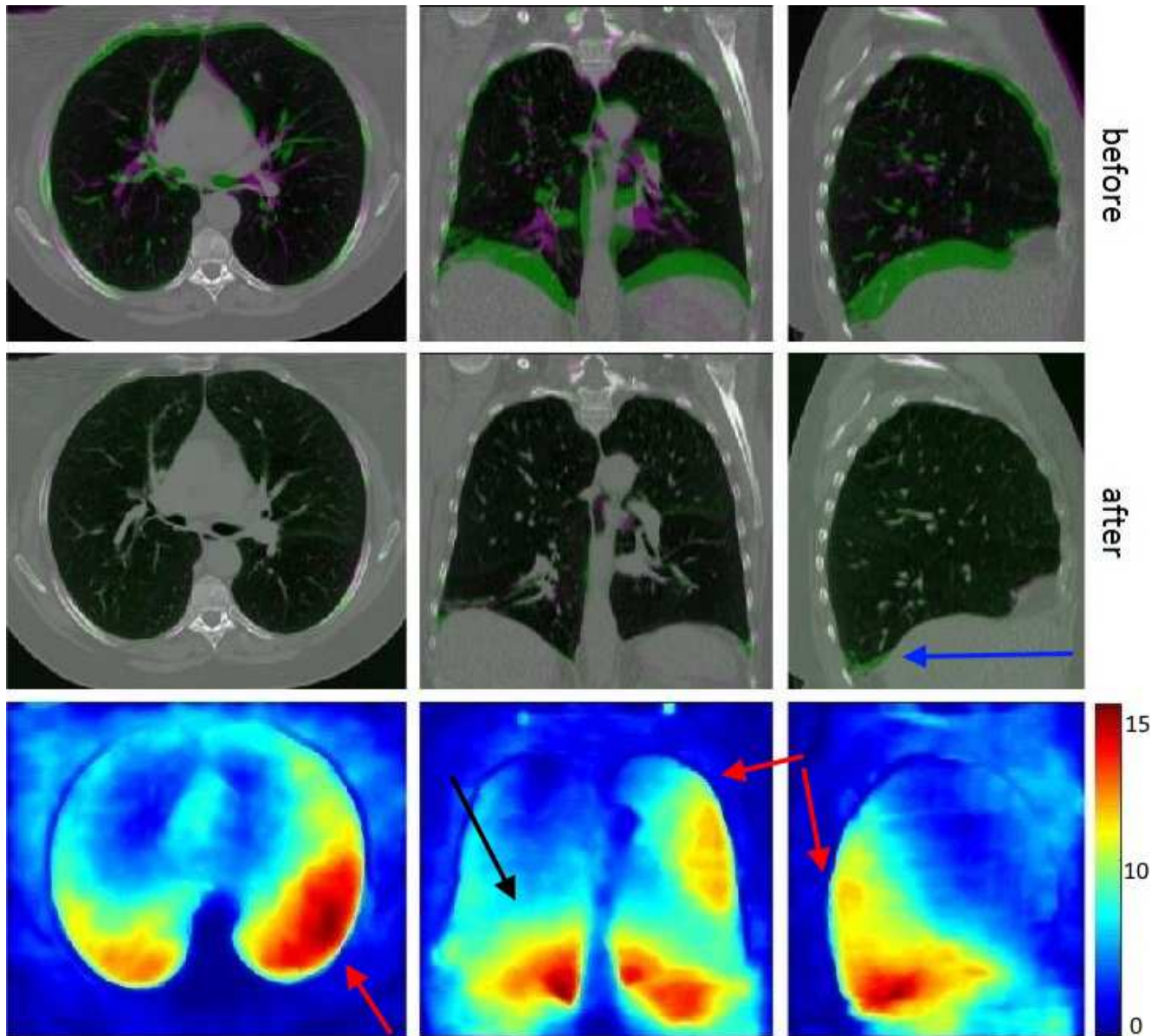


Figure 3. Registration results for the proposed method for the most challenging Dir-Lab case 8 in axial, coronal and sagittal view. In the upper row an overlay of full inhale (green) and full exhale (magenta) is presented. In the middle row the same slices after performing the proposed registration are shown. The initial misalignment, visible in the upper row as shadows in green and magenta, is almost completely eliminated after the registration. In the bottom row the magnitude of the displacement field in mm is presented, with well visible ‘sliding’ motion in all views pointed at by red arrows. The black arrow points at clear change in the magnitude of the displacement, which displays good correspondence with anatomical border between lung lobes.

0.85. To calculate the MIND descriptor, six neighbouring voxels were used. The graph cuts optimization was performed until convergence.

In Table 1 we show the results for applying our technique to the Dir-Lab dataset, in comparison to the most closely related continuous optimization-based Demons registration method using bilateral filtering (BLF [24]), as well as two other state-of-the-art methods using discrete

optimization-based registration: MST-based belief propagation (deeds [17]) and supervoxel-based belief propagation (SBP [18]). We used the Target Registration Error (TRE) to quantify the accuracy of the registration methods. The proposed method achieves an average TRE of $1.18 \pm 0.8mm$, whereas the mean TRE for Demons-based bilateral filtering is $1.95 \pm 0.7mm$. Applying the two discrete optimization-based methods, deeds and supervoxel-based belief prop-

agation, resulted in mean TREs of $1.43 \pm 1.3mm$ and $1.23 \pm 0.8mm$, respectively.

The visualization of the errors distribution for case 8, the most challenging, is shown in Figure 2, with the visual registration result shown in Figure 3. Red arrows point to visible preservation of ‘sliding’ motion at the lung boundaries. Some artefacts can be noticed at the lowest regions of the lungs, as can the misalignment in the coronal view, marked by the blue arrow. Quite interesting is the clearly visible change in the magnitude of the displacement field marked by the black arrow in the coronal view. The change corresponds to a fissure between lung lobes.

5. Discussion

The presented results for our method show that, even though for each of the supervoxels a discrete displacement vector is assigned, the application of image-guided filtering is capable of providing a locally continuous deformation field, at the same time preserving ‘sliding’ motions. In terms of accuracy, our method outperforms both continuous and discrete optimization-based counterparts. However, in our formulation we used MIND as a similarity measure, whereas in BLF [24] normalised gradient fields were applied, which could affect comparisons. Graph relaxation, which can be considered as partial segmentation, also could have a strong influence on the results. The proposed method slightly outperformed supervoxel-based belief propagation (SBP) [18], where multiple layers of supervoxels were used.

Of the compared registration methods, the supervoxel-based methods: the proposed and SBP show noticeable improvement over continuous Demons-based method and the regular grid discrete optimization-based (deeds). Nevertheless, the artefacts observed for our method that are highlighted in Figure 3, which could be caused by the graph relaxation, require further investigation. Additionally, in the proposed framework the number of voxels within a single supervoxel at the second highest resolution level is relatively high, in comparison to other levels, and we predict that clustering the image into smaller subsets could further improve the results. This problem is partially compensated at the highest resolution level at the expense of the region search size. In comparison to the voxel-based graph cuts method, the proposed formulation based on supervoxels allows for a much less complex problem to be solved.

6. Conclusions

In this paper, we have shown that graph cuts-based registration can be successfully applied to lung registration. The reduction in the complexity of the optimization problem by using a supervoxel image representation not only enables the method to run in reasonable time (our sub-optimal Matlab implementation takes about an hour per volume) but

also, when combined with a relaxed graph representation and image-guided filtering, helps to preserve lung ‘sliding’ motion and improve modeling of complex lung breathing motions. Moreover, the results after applying the proposed method on the Dir-Lab dataset suggest that our framework using graph cuts on a relaxed graphs performs favourably in comparison to state-of-the-art methods, even slightly outperforming in average the best of them in the terms of overall accuracy - supervoxel-belief propagation method [18].

A more detailed analysis, including testing different similarity measures and more data sets as well as multi-modal data, is needed. An additional comparison between bilateral filtering and guided image filtering applied to our formulation would give a more detailed view in the performance of the both method. Instead of a fixed threshold in a graph relaxation step, a sigmoid function could be used and we plan to evaluate such a potential solution. Nevertheless, substituting continuous optimization with its discrete-based counterpart in the proposed image-guided filtering approach is an attractive and computationally tractable improvement.

7. Acknowledgments

We would like to acknowledge funding from the CRUK/EPSRC Oxford Cancer Imaging Centre.

References

- [1] R. Achanta, A. Shaji, K. Smith, A. Lucchi, P. Fua, and S. Süsstrunk. SLIC superpixels compared to state-of-the-art superpixel methods. *IEEE Trans. Pattern Anal. Mach. Intell.*, 2012.
- [2] B. Avants and a. J. G. C. Epstein, M. Grossman. Symmetric diffeomorphic image registration with cross-correlation: Evaluating automated labeling of elderly and neurodegenerative brain. *Med. Image Anal.*, 12:26–41, 2008.
- [3] H. Y. Baluwala, L. Rissler, J. A. Schnabel, and K. A. Saddy. Toward physiologically motivated registration of diagnostic CT and PET/CT of lung volumes. *Med. Phys.*, 40(2):021903, 2013.
- [4] Y. Boykov and G. Funka-Lea. Graph cuts and efficient N-D image segmentation. *Int. J. Comput. Vis.*, 70(2):109–131, 2006.
- [5] Y. Boykov and V. Kolmogorov. An experimental comparison of min-cut/max-flow algorithms for energy minimization in vision. *IEEE Trans. Pattern Anal. Mach. Intell.*, 26:1124 – 1137, 2004.
- [6] Y. Boykov and O. Veksler. Graph Cuts in Vision and Graphics: Theories and Applications BT - Handbook of Mathematical Models in Computer Vision. *Handbook of Mathematical Models in Computer Vision*, (Chapter 5):79–96, 2006.
- [7] Y. Boykov, O. Veksler, and R. Zabih. Fast approximate energy minimization via graph cuts. *IEEE Trans. Pattern Anal. Mach. Intell.*, 23(11):1222–1239, 2001.
- [8] R. Castillo, E. Castillo, R. Guerra, V. E. Johnson, T. McPhail, A. K. Garg, and T. Guerrero. A framework for evaluation of

- deformable image registration spatial accuracy using large landmark point sets. *Phys. Med. Biol.*, 54(7):1849–1870, 2009.
- [9] R. Castillo, E. Castillo, and T. Guerrero. Ventilation from four-dimensional computed tomography: density versus Jacobian methods. *Phys. Med. Biol.*, 55:4661–4685, 2010.
- [10] M. Chen, W. Lu, Q. Chen, K. J. Ruchala, and G. H. Olivera. A simple fixed-point approach to invert a deformation field. *Med. Phys.*, 35(1):81–88, 2008.
- [11] P. F. Felzenszwalb and D. P. Huttenlocher. Efficient belief propagation for early vision. *Int. J. Comput. Vis.*, 70(1):41–54, May 2006.
- [12] B. Glocker, N. Komodakis, G. Tziritas, N. Navab, and N. Paragios. Dense image registration through MRFs and efficient linear programming. *Med. Image Anal.*, 12(6):731–741, 2008.
- [13] B. Glocker, A. Sotiras, N. Komodakis, and N. Paragios. Deformable Medical Image Registration: Setting the State of the Art with Discrete Methods. *Annu Rev Biomed Eng*, 13:219–244, 2011.
- [14] K. He, J. Sun, and X. Tang. Guided Image Filtering. *IEEE Trans. Pattern Anal. Mach. Intell.*, 35(6):1397–1409, 2013.
- [15] M. P. Heinrich, H. Handels, and I. J. A. Simpson. Estimating large lung motion in COPD patients by symmetric regularised correspondence fields. *Med. Image Comput. Comput.-Assist. Intervent. (MICCAI 2015)*, 9350:338–345, 2015.
- [16] M. P. Heinrich, M. Jenkinson, M. Bhushan, T. Matin, F. V. Gleeson, M. Brady, and J. A. Schnabel. MIND: modality independent neighbourhood descriptor for multi-modal deformable registration. *Med. Image Anal.*, 16(7):1423–1435, Oct. 2012.
- [17] M. P. Heinrich, M. Jenkinson, M. Brady, and J. A. Schnabel. MRF-based deformable registration and ventilation estimation of lung CT. *IEEE Trans. Med. Imag.*, 32(7):1239–1248, July 2013.
- [18] M. P. Heinrich, I. J. Simpson, B. W. Papież, S. M. Brady, and J. A. Schnabel. Deformable image registration by combining uncertainty estimates from supervoxel belief propagation. *Med. Image Anal.*, 27:57–71, 2016.
- [19] R. M. Kaus, T. Netsch, S. Kabus, V. Pekar, T. McNutt, and B. Fischer. Estimation of Organ Motion from 4D CT for 4D Radiation Therapy Planning of Lung Cancer. *Med. Image Comput. Comput.-Assist. Intervent. (MICCAI 2004)*, 3217:1017–1024, 2004.
- [20] H. Lombaert, Y. Sun, and F. Chriet. Landmark-based Non-rigid Registration via Graph Cuts. *Lec. Notes Comput. Sc.*, 2007.
- [21] J. Modersitzki. *Numerical Methods for Image Registration*. 2004.
- [22] K. Murphy, B. Van Ginneken, J. M. Reinhardt, S. Kabus, K. Ding, X. Deng, K. Cao, K. Du, G. E. Christensen, V. Garcia, T. Vercauteren, N. Ayache, O. Commowick, G. Malandain, B. Glocker, N. Paragios, N. Navab, V. Gorbunova, J. Sporring, M. De Bruijne, X. Han, M. P. Heinrich, J. A. Schnabel, M. Jenkinson, C. Lorenz, M. Modat, J. R. McClelland, S. Ourselin, S. E. A. Muenzing, M. a. Viergever, D. De Nigris, D. L. Collins, T. Arbel, M. Peroni, R. Li, G. C. Sharp, A. Schmidt-Richberg, J. Ehrhardt, R. Werner, D. Smeets, D. Loeckx, G. Song, N. Tustison, B. Avants, J. C. Gee, M. Staring, S. Klein, B. C. Stoel, M. Urschler, M. Werlberger, J. Vandemeulebroucke, S. Rit, D. Sarrut, and J. P. W. Pluim. Evaluation of registration methods on thoracic CT: the EMPIRE10 challenge. *IEEE Trans. Med. Imag.*, 30(11):1901–1920, 2011.
- [23] B. W. Papież, J. Franklin, M. P. Heinrich, F. V. Gleeson, and J. A. Schnabel. Liver Motion Estimation via Locally Adaptive Over-Segmentation Regularization. *Med. Image Comput. Comput.-Assist. Intervent. (MICCAI 2015)*, 9351:427–434, 2015.
- [24] B. W. Papież, M. P. Heinrich, J. Fehrenbach, L. Risser, and J. A. Schnabel. An implicit sliding-motion preserving regularisation via bilateral filtering for deformable image registration. *Med. Image Anal.*, 18(8):1299–311, Dec. 2014.
- [25] L. Risser, F. X. Vialard, H. Y. Baluwala, and J. A. Schnabel. Piecewise-diffeomorphic image registration : application to the motion estimation between 3D CT lung images with sliding conditions. *Med. Image Anal.*, 17(2):182–193, 2013.
- [26] D. Rueckert, L. I. Sonoda, C. Hayes, D. L. Hill, M. O. Leach, and D. J. Hawkes. Nonrigid registration using free-form deformations: application to breast MR images. *IEEE Trans. Med. Imag.*, 18(8):712–21, Aug. 1999.
- [27] J. Ruhaak, S. Heldmann, T. Kipshagen, and B. Fischer. Highly accurate fast lung CT registration. *SPIE Med. Imag.*, 86690Y, 2013.
- [28] A. Schmidt-Richberg, R. Werner, H. Handels, and J. Ehrhardt. Estimation of slipping organ motion by registration with direction-dependent regularization. *Med. Image Anal.*, 16:150–159, 2012.
- [29] R. W. K. So and A. C. S. Chung. Non-rigid image registration by using graph-cuts with mutual information. *IEEE Image Proc.*, Sept(1522-4880):4429–4432, 2010.
- [30] R. W. K. So and A. C. S. Chung. Learning-based non-rigid image registration using prior joint intensity distributions with graph-cuts. *IEEE Image Proc.*, 2:717–720, 2011.
- [31] R. W. K. So, T. W. H. Tang, and A. C. S. Chung. Non-rigid image registration of brain magnetic resonance images using graph-cuts. *Pattern Recognit.*, 44(10-11):2450–2467, 2011.
- [32] T. W. H. Tang and A. C. S. Chung. Non-rigid image registration using graph-cuts. *Med. Image Comput. Comput.-Assist. Intervent. (MICCAI 2007)*, 10(Pt 1):916–924, 2007.
- [33] C. Tomasi and R. Manduchi. Bilateral Filtering for Gray and Color Images. *Int. J. Comput. Vis.*, pages 839–846, 1998.
- [34] J. Vandemeulebroucke, O. Bernard, S. Rit, J. Kybic, P. Clarysse, and D. Sarrut. Automated segmentation of a motion mask to preserve sliding motion in deformable registration of thoracic CT. *Med. Phys.*, 39, 2012.
- [35] T. Vercauteren, X. Pennec, A. Perchant, and N. Ayache. Diffeomorphic demons: efficient non-parametric image registration. *NeuroImage*, 45(1 Suppl):S61–S72, 2009.
- [36] E. Weiss, K. Wijesooriya, S. V. Dill, and P. J. Keall. Tumor and normal tissue motion in the thorax during respiration: Analysis of volumetric and positional variations using 4D CT. *Med. Image Comput. Comput.-Assist. Intervent. (MICCAI 2004)*, 67:296307, 2007.